Impact and usage of the shear thickening fluid (STF) material in damping vibration of bolted flange joints

OPEN ACCESS
IOP Publishing
Smart Materials and Structures
Smart Mater. Struct. **28** (2019) 095005 (10pp)
https://doi.org/10.1088/1361-665X/aaef6c

Impact and usage of the shear thickening fluid (STF) material in damping vibration of bolted flange joints

Yacong Guo[1,2,3], Yanpeng Wei[1,2], Jinlong Zou[1], Chenguang Huang[2], Xianqian Wu[2], Zishang Liu[2,3] and Zhe Yang[2]

[1] Science and Technology on Electromechanical Dynamic Control Laboratory, Xian 710065, People's Republic of China
[2] Key Laboratory for Mechanics in Fluid Solid Coupling Systems, Institute of Mechanics, Chinese Academy of Sciences, Beijing 100190, People's Republic of China
[3] School of Engineering Science, University of Chinese Academy of Sciences, Beijing, 100049, People's Republic of China

E-mail: weiyanpeng@imech.ac.cn

Received 29 June 2018, revised 21 October 2018
Accepted for publication 8 November 2018
Published 31 July 2019

Abstract

Bolted flange joints in fuzes undergo high acceleration during penetration, along with nonlinear responses which are forced reaction, structural vibrations, and shock effects. Vibrations of high frequencies aggregate noises and make it harder for the signal processing of fuzes. This study proposed an effective and innovative method of suppressing vibrations of high frequencies caused by impact loading. Shear thickening fluids (STFs) were stuffed into bolted flange joints. A damper of 57 vol/vol% dense silica particle-ethylene glycol suspension was inserted into gaps between the surfaces of the incident bar and the flange. Based on a modified split Hopkinson pressure bar, pulse widths, amplitudes, and structural frequencies of both impact and vibrational response regions were evaluated to examine the effectiveness of the STF damper. The amplitude and pulse width in the vibrational response region were significantly reduced, since this suspension forms jamming clusters subjected to impulses, attenuating the shockwaves. The STF fillers under various lengths of projectiles from 50 mm–400 mm were discussed to validate effectiveness. Further comparisons with epoxy resin fillers with various curing times indicated that the STF inhibited high frequency oscillations as a protector, and damped the dominant frequency of the original structure. However, experimental data showed that the transmission pulse of the incident bar was similar to joints without protection, indicating that the force transmission ratio was not affected by the fillers. These results show the feasibility of STFs as energy absorbers for vibration reduction of bolted flange joints.

Keywords: shear thickening fluid, bolted flange joints, energy dissipation, vibration suppression

(Some figures may appear in colour only in the online journal)

1. Introduction

Bolted flange joints are widely used to connect large engineering structures such as pipes and aircraft, especially for fuzes of projectile penetration. They generate vibrations of high frequencies due to impact loading. Because of their complex geometry and multi-material properties, the response is nonlinear under impact [1]. For traditional dynamic loads,

the response comprises only forced and structural vibrations. Meanwhile, the duration of the forced vibrations is the same with excitation. Impacts caused by penetration typically reach hundreds of MPa, with pulse widths ranging from tens to hundreds microseconds. When the joint is subjected to these impacts, the forced vibration is nonlinear and the shock effect is significant [2]. The frequency of response is changed from that of the excitation, which is characterized by the force transmission ratio α. The resistance to impact and material damping is critical for space, military, and industrial applications subjected to dynamic loading. Dampers should offer protection for the internal conductors, actuators, and circuits that experience impact shocks and vibration. In this study, we propose an optimal damper that can suppress high frequency vibrations to provide protection, decrease structural noise, and provide a clean environments for data recording [3].

Protection for fuzes concentrates primarily on structural optimization, strengthening the actuators, and isolating environmental disturbances. Limited space inside fuzes restricts energy dissipation under impacts. Energy dissipation through a medium is a straightforward method, and is extensively used in numerous fields. Nowadays, cushioning materials in fuzes are typically polyurethane foams, rubber, or industrial blankets. Polyurethane foams find wide application as they can dissipate impact energy while distributing the impact forces over the surface of the supporting structures, especially oblique impacts [4]. Rubber exhibits significant low wave-speeds and perfect dilatability [5], effectively attenuating direct impacts [6]. However, although many additional cushions absorb impact energy and protect devices, the suppression of subsequent vibrations is still unclear. In some cases, these materials can even introduce high frequency noises. The electronic parts in fuzes, recording the progress of penetration, are susceptible to ambient noise. Therefore, cushioning materials need to be capable of resisting impacts as well as reducing oscillations. The impact resistance of these materials lose their efficiency partially, or on occasion completely, after a single significant impact. Automotive shock absorbers, dedicated, fluid-filled dampers can be used to absorb unwanted energy [7]. Fluidic damping has the advantage that energy dissipation occurs continuously in a limited space, so that undesirable oscillations are efficiently suppressed.

A shear thickening fluid (STF) is a dense suspension of colloidal particles scattered in a carrier fluid [8] exhibits reversible energy absorption behavior [9–11]. STFs recover rapidly when the shear rate or shear stress is removed [12]. Numerous experts have conducted rheological studies to investigate the effect of shear thickening of such suspensions [13–15]. The distinct viscosity is accurately controlled by loading conditions, specifically at high strain rates. Previous studies concentrated on interpreting the mechanism of STFs subjected to various pressures and strain rates [16]. Jiang reported that the stress pulse energy decayed rapidly when propagated through STFs in SHPB tests [10]. When compared to an ethylene glycol solution, the amplitude of transmission pulse through STFs was significantly smaller, and the pulse width was greater. Wu [17] examined the dynamic response of STFs subjected to laser induced shocks with peak pressures in the order of several gigapascal. Later, the team studied the attenuation behavior of shock waves in STFs [18]. These studies confirmed that STFs have the capacity to dissipate energy when subjected to extreme loads.

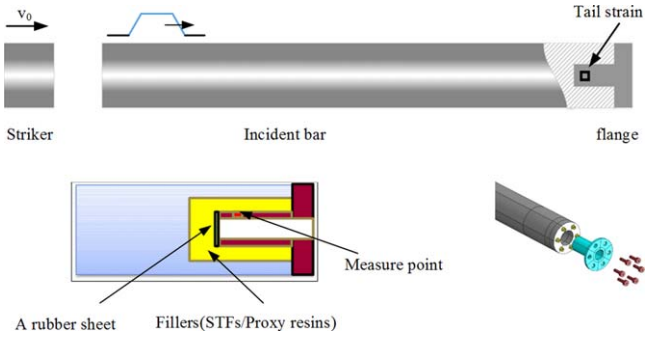

Figure 1. Revised SHPB setup.

Therefore, STFs are widely used in dampers [19] and body armors [20–23]. Furthermore, scientists pay much attention on integrating adaptive materials into composite structures to better control vibration and stiffness [7, 24, 25]. Integrating the STF core in a sandwich beam can reduce the vibrations of the beam [25]. However, the excitation frequency was limited to approximately 40 Hz. A passively damped micro-electro-mechanical system (MEMS) device is proposed, and the damping increases significantly when the device is subjected to a high amplitude driving force [3]. However, the driving force was torsional loading and only reached several hundreds of μN. In fact, joints oscillated significantly during hydro velocity penetration [26]. To date, resistance to extreme impact, typically pulse widths of microseconds and amplitudes of several hundred MPa, have not been considered.

With this motivation, an experimental method is proposed to investigate the response of a bolted flange joint stuffed a STF layer subjected to shockwaves. Various pulse widths achieved at the SHPB platform are used to evaluate the effect of vibrational suppression. The original joint without fillers, and with epoxy resin protectors in the same structure, are also discussed. Our study proposes a design of energy absorbers in large engineering structures subjected to extreme loading conditions.

2. Experimental method

The split Hopkins pressure bar (SHPB) setup is commonly used for analyzing dynamic mechanics. In figure 1, a flange is attached to the incident bar by six M4 bolts, and the tail of the suspended body is sealed by a rubber sheet. In this study, the key parameters are the axial strain of the flange, and its frequency. Therefore, the transmitted bar is removed. The behavior of flanges without fillers under shockwaves has been comprehensively studied previously [2]. The space between the flange and the incident bar is filled with STFs or epoxy resins, shown in the yellow part of figure 1. Two types of

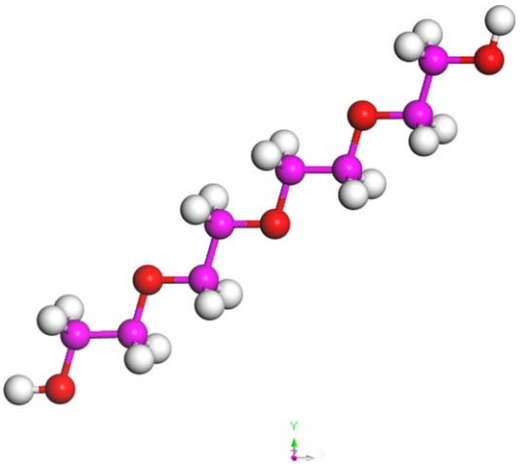

Figure 2. The diagram of PEG200.

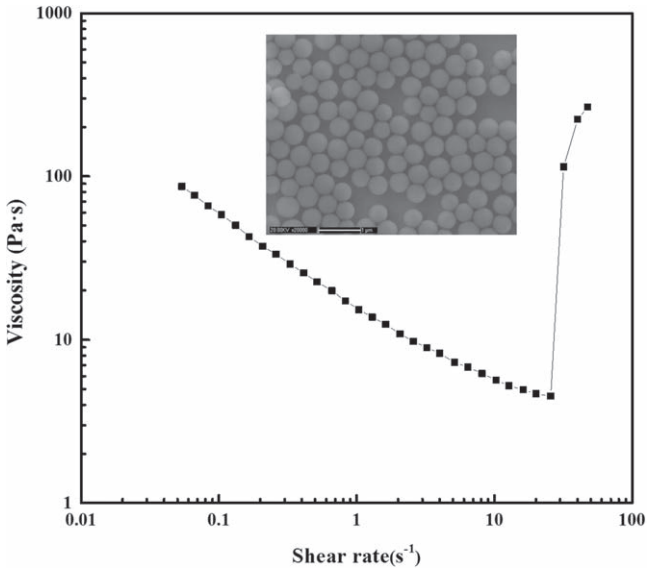

Figure 3. Steady state shear viscosity of STFs at various strain rates.

strain gages are used in this study, standard gages and semiconductors. The signals are recorded at a sampling frequency of 5 MHz. All of the signals transformed by Wheatstone bridge circuits are amplified using a differential amplifier (Tektronix 5A22N), and then recorded on a digital oscilloscope (Tektronix TDS 420).

The STF comprises a stabilized dispersion of rigid submicrometer particles in a natural carrier fluid, exhibiting a significant increase on viscosity. In this study, it is a colloidal dispersion of 57% (by weight) fumed silica nanoparticles in a polyethylene glycol (PEG) solvent. The silica nanoparticles are dispersed into the PEG solvent by hand mixing and an ultrasonic vibrator, achieving an ordered dispersion average of 300 nm, with less than 10% polydispersity. In this paper, we choose PEG200 as the solvent see figure 2, and the molecular weight is 194.227. The densities of silica nanoparticles and PEG are $1.950\,\mathrm{g\,cm^{-3}}$ and $1.127\,\mathrm{g\,cm^{-3}}$ respectively. For polyethylene glycols, the speed of sound is $1650\,\mathrm{m\,s^{-1}}$ (with $E_{PEG} = 3.05$ GPa). The flow rate of the STF was measured by a Kinexus pro + rotational rheometer in the steady-state shear sweep mode, using a 40 mm 4° cone and plate, with Peltier temperature control at 25 °C. A typical plot of viscosity versus shear rate is shown in figure 3. It indicates a strong shear thickening response at shear rates of $25–60\,\mathrm{s^{-1}}$ after a shear thinning phenomenon.

Micro-scale devices are embedded with cushioning materials, such as epoxy resins. To highlight the advantages that STFs offer in industrial structures, epoxy resins are used in this study. They have approximately the same density and viscosity as STFs. The epoxy resin (Caster HL-1112, manufactured by HASUNCAST in China) mainly comprises a combination of araldite 506 (CAS No. 25068-38-6) and alkyl (C12-C14) glycidyl ether (CAS No. 68609-97-2). According to the manufacturer, the mix ratio (parts by weight) is 2:1, labeled as Parts A and B respectively in table 1. The mixed fluid, with the same density as the STF, has an original viscosity of 2 Pa · s. It is obviously less than that of STF. Numerous studies on the relationship between viscosity and curing time of epoxy resins have shown that curing at 40 °C for 2 h is required to achieve fully curing [27–29]. It is

Table 1. Detailed properties of HL-1112 before mixing.

Components	Part A	Part B
Density ($\mathrm{g\,cm^{-3}}$)	1.16	1.09
Original viscosity (Pa · s)	2.6	1.5
Mixing weight ratio	2	1

commonly acknowledged that the rheological properties are determined by the shear history, temperature, and flow geometry [30]. According to Kiuna [28], it is optimal to cure the epoxy resin for 1 h, as it attains to the same level of viscosity as STF. We also studied the mixture every 30 min intervals during the curing process.

Before the test, STFs and various epoxy resin mixtures were inserted into the space between the flange and incident bar, as shown in figure 4. Since fillers are highly viscous, once the bolts are tightened, no fluids leak out. The diameter of the flange is 37 mm. The incident bar has variable cross-sections, and its diameter ranges from 23–37 mm. Five projectile lengths are used, that is 50 mm, 100 mm, 200 mm, 300 mm, and 400 mm. They can reach the loading velocities of $7–14\,\mathrm{m\,s^{-1}}$. Detailed information of the loading conditions is presented in table 2. After each test, the structure of the bolted flange joints should be cleaned by acetone in order to ensure identical original surface states. All the test are taken at the room temperature, 20 °C. Although the viscosity may decreases as the temperature rises, the shear thickening phenomenon still remains as figure 5. However, the critical point of shear thickening is elevated. It means more shear rates are needed when the temperature goes up. Therefore, we believe that STFs can remain its capacity of damping at higher temperatures. In this paper, we only consider the ordinary room temperature from 0 °C to 20 °C and it covers the work temperature of most fuzes applications. The strain signals, under various impact velocities and pulse widths, are

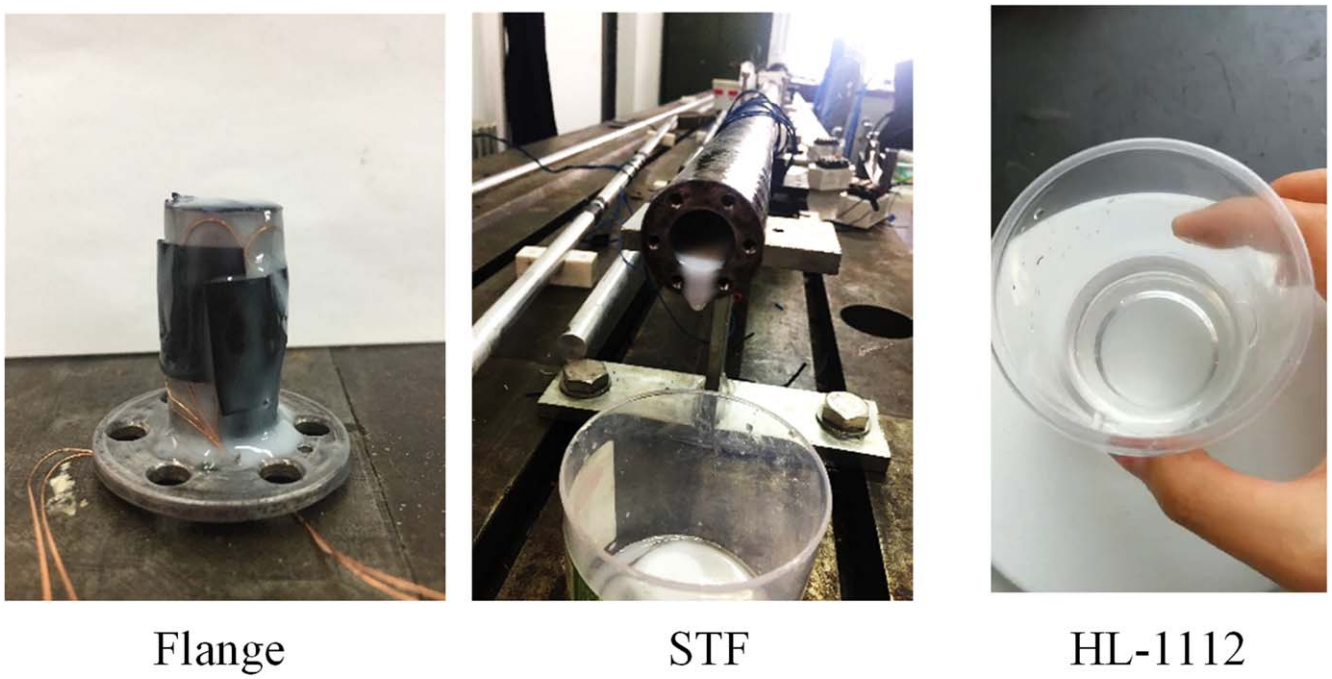

Figure 4. Filler (STFs and proxy resins) used in experiments.

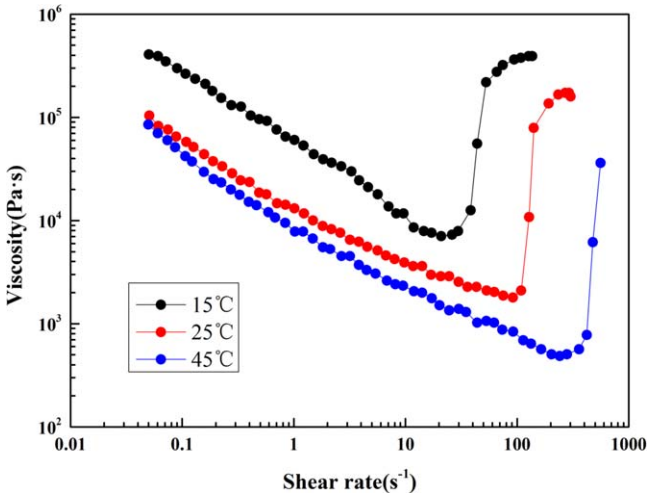

Figure 5. The relationship of viscosity and shear rate at different temperature.

recorded in order to compare the impact resistance of different fillers.

3. Results and discussion

The conventional dynamic response theory of linear systems under impulse includes forced vibrations and structural vibrations. As the joint contains discontinuous interfaces and different stiffness under tension and compression, attenuation of excitation and energy dissipation cannot be ignored. Many efforts have been made to identify the friction of the joints, predicting the nonlinear behavior [20]. However, its configuration is only suitable for a single bolt under dynamic loading. Our previous study developed a revised dynamic response theory for joints as a whole system. Base on the spectral formation [31], the response of bolted flange joints contained three physical phenomena, forced vibration, structural vibration, and shock response, and can be expressed as follows:

$$\frac{A}{A_0} = A_d \sin(\omega_d t/\alpha) + A_n \sin \omega_n t + A_s \sin \omega_s t$$
$$\omega_d = \pi/T_d,\ \ \omega_n = 2\pi/T_n,\ \ \omega_s = 2\pi/T_s \qquad (1)$$

where T_d is the duration of excitation, T_n is the natural period, T_S is the period of the shockwave in the flange, and ω corresponds to the radical frequency. We used transmission ratio α, the duration of impact response region T_p to the pulse width T_d, to describe the nonlinear response of flange structures. Shockwaves might dissipate and damp coming across the joint, and the frequency of response decreased comparing to the loading one. Therefore, the transmission ratio is considered as the characteristic of nonlinearity. The dynamic response was evaluated by the duration and amplitude.

3.1. Comparison of original joint and joints with STFs/epoxy resin fillers

Stress waves in the incident bar fired by the 300 mm projectile are shown in figure 6. The loading curves coincide precisely with each other, indicating the same loading conditions. Three configurations are tested. The original flange structure without any filler is labeled as 'air', while the joint filled with shear thickening fluids is labeled as 'STF' and 'HL-1112' represents the joint with epoxy resin stuffing. Traditional theory for linear system under impact loading contains two region, forced vibration and structural vibration. The response is divided into two region as shown in figure 7, that is impact response region and vibrational response region. Stress waves

Table 2. Loading condition of experiments with single pulse width.

Experimental code	112-1	112-2	112-3	112-5	112-10	111-1	111-2	111-3	113-4
Pressure (MPa)	0.16	0.15	0.20	0.25	0.30	0.20	0.2	0.2	0.25
Impact velocity ($m\,s^{-1}$)	6.40	6.52	7.32	6.86	9.56	1178	11.06	12.10	13.76

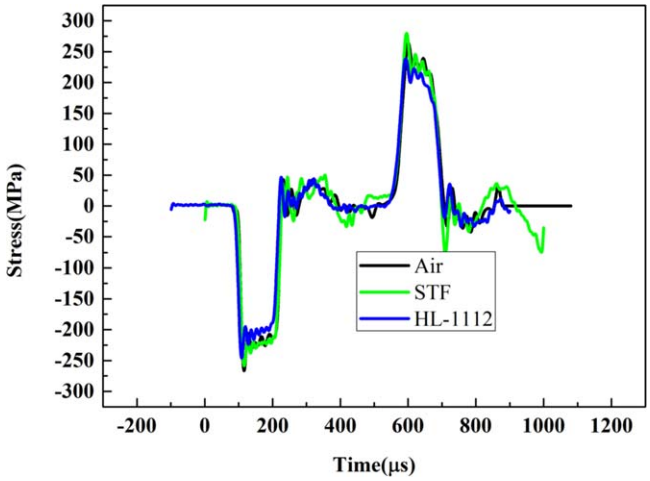

Figure 6. Stress waves of 300 mm projectile impacting incident bar.

spread through the bar from one end to the other. The shock wave will dissipate and reflect back, coming across the joint. The damping of the joint leads to the nonlinear response, and the change of waves is recorded in the reflected waves. Therefore, the pulse width of the reflected waves in the bar is the duration of impact response region. It means the joint experience the process of impact loading. After that, there is a vibrational response region. The peaks of vibrational response region decreases as a form of exponential line. Finally, the damping curve shown in figure 5 intersects with ambient noise. Therefore, the point of intersection is the end of the vibrational response region. Although the structures have a few differences, the durations of the reflected waves are similar, approximately 170 μs. It suggests that the force transmission ratio is not affected by the fillers.

The energy acquired by structures comes from the difference between the incident energy and the reflected one. For the original flange structure, without fillers, all the energy spreads into the flange. On the contrast, the fillers absorb a portion of the energy in the others. Detailed comparative data is presented in table 3. The structures without fillers acquired the least energy, 0.16 J. However, the energies received in cases with STFs and epoxy resin, reach 0.49 J and 0.32 J respectively. Without fillers as protections, shockwaves propagate along the bolt screw into the flange, leading to oscillation of the flange. In contrast, since STFs or epoxy resin fillers are low impact resistance materials, they attenuate the waves. Both wave speeds are relatively smaller than that in steel. Increased viscosity results in increased damping. The convincing statement is the jamming particle cluster theory, that is an ordered arrangement of particles change states to a disordered one [32]. Furthermore, additional fillers add new propagation paths for the excitation, leading to greater energy absorbed in the structure. Amplitudes of both regions are listed in table 3. In the case of STF, the amplitude of the impact response region is clearly smaller than others, only 71.88 micro-strain. It means the STF works as a damper, effectively preventing the vibration of flange and diminishing the amplitude.

Signals in the vibrational response region indicate STFs have a significant effect on reducing vibrations. As can be seen in figure 7, the original structure without fillers has a wave pulse of 273.0 μs, and the HL-1112 case (filled with epoxy resin) 334.2 μs. However, the pulse width of the STF case is prominently reduced to 180.5 μs. According to our previous study, the natural frequency of flange without fillers is 11 KHz and the frequency responded to the duration of shockwave is about 70 KHz. Signals in the impact response region comprised the response to excitations and shock behavior. Structural vibration together with shock behavior (approximately 70 kHz) comprise the signal of the vibrational response region. The STF case effectively changes the vibrational characteristics in the vibrational response region other than in the impact response region. STFs inhibit the wave-spread in the flange. Fast Fourier transform (FFT) spectrums of axial strains in figure 8 also confirm that. The air case emerges two significant frequencies, the natural frequency (approximately 11 kHz), and the shock response. There are several peaks nearly at the same level in the HL-1112 case. The vibration at natural frequency is still prominent. Therefore, the epoxy resin as a protector can neither change the structural frequency, nor eliminate oscillations of high frequencies. It only damps the amplitude to some extent. In comparison, the dominant frequency of the STF case is 7 kHz, which is significantly lower than the others. Above 15 kHz, the curve is typically damped asymptotically toward zero. Under high shear rates primarily driven by shockwaves, the STF changes its state from a fluid-like to a solid-like material, but the epoxy resin does not exhibit changeable rheological properties. In conclusion, the STF as an energy absorber not only inhibits the shock effect, but also damps the basic frequency. STFs can be used as protectors for fuzes. When MEMS in fuzes is subjected to impact, STFs will help them filtering noise, especially oscillation of high frequency, and remain the signal of impact clearly at the same time.

3.2. Comparison of STF and epoxy resins at different curing times

The mechanical properties of epoxy resins may change during the solidification process. With time the viscosity increases until the fluid mixture turns into a gel state, similar to a transparent jelly. It is difficult to accurately measure the viscosity during the curing process under the current

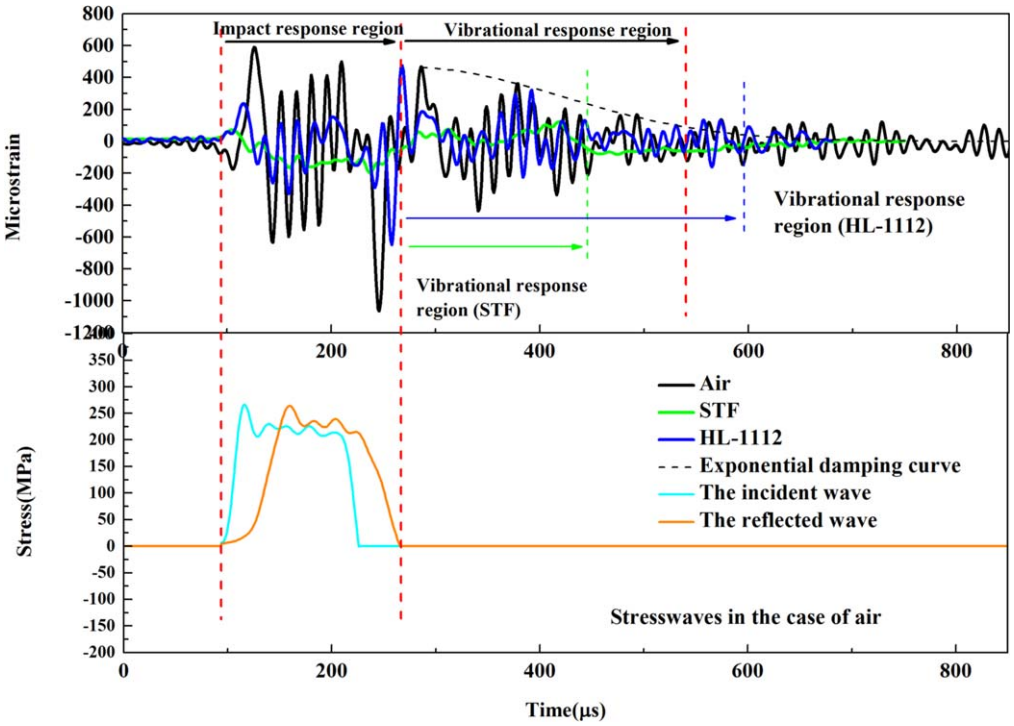

Figure 7. Comparison of axial strain in flange for three cases: original flange, and flanges with STF and proxy resin (HL-1112) fillers.

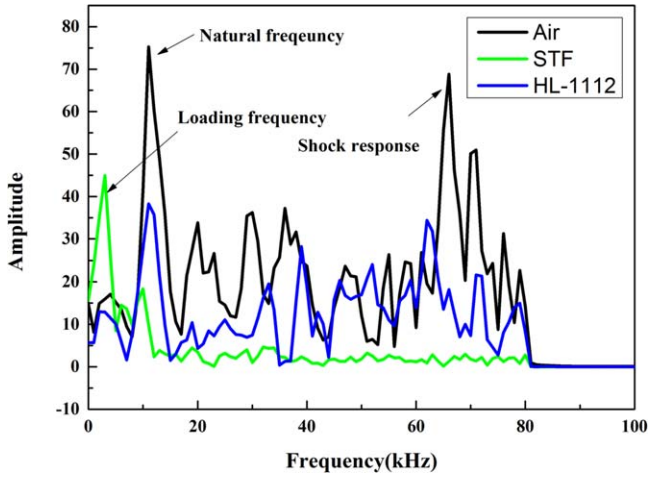

Figure 8. FFT spectrum for three cases: original flange structure, and STF and proxy resin (HL-1112) filers.

experimental conditions. A number of epoxy resins at different curing time were tested to prove the advantage of STFs on suppressing vibration. These cases covered various viscosity of epoxy resins. Although the epoxy resin was selected as a reference, the initial mixture seldom had a low density and high viscosity simultaneously. After each 30 min of curing time, the samples were inserted into the empty space of the flange. For the case of 100% cure, the mixture was inserted as it turned into a gel-like state. The experiments were started once the epoxy had completely solidified. A 1 h-sample of epoxy resin has the approximate physical state of STFs. The stress wave of the 300 mm projectile impact is shown in figure 9. The reflected waves are essentially similar, indicating that curing time has no influence on the transmission ratio. Axial strains of different curing times are shown in figure 10. The middle state, one hour curing time, exhibits the worst oscillations. The amplitude shifts significantly. When the epoxy resin is fully cured, the vibration is more moderate and the amplitude decreases. Therefore, after solidification epoxy resins behavior like a rubber material, significantly more effective at absorbing energy and attenuating shockwaves.

The FFT spectrums of different curing times are shown in figure 11. The dominant frequencies remain 11 kHz for both the 30 min and 1 h cases, while the base frequency increases to 30 kHz in the fully curing case. That agrees well with previous studies [24]. The natural frequency of sandwich structure with Epoxy resins layer increased after curing. Epoxy resin is not able to eliminate oscillations of high frequencies, and instead introduces extra undesired noise after solidification. Furthermore, only STFs decrease the structural frequency and inhibits vibrations of high frequency. Therefore, the STF is the best absorber when compared to proxy resins at different curing states. In order to reduce vibrations in engineering structures, STFs are recommended to replace the epoxy resin as an embedding material.

3.3. Comparison of STFs under various pulse widths

Comparisons of flange with STFs under various impact loading is discussed in this section. The lengths of projectiles are 50, 100, 200, 300 and 400 mm. Since the pulse width of loading is different, ranging from 45–190 μs, the duration of impact response region consequently is distinct. Thus, we do not discuss the duration of impact response region. Amplitudes in both the impact and vibrational response regions exhibit similar behavior. In table 4, the maximum amplitudes

Table 3. Detailed experimental data of three structures under 300 mm projectile impacts.

Case	Air	STF	HL-1112
Incident energy (J)	12.36	11.28	10.70
Energy achieved in flange structure (J)	0.16	0.49	0.32
Duration of dynamic response (μs)	445.5	350.5	501.4
Duration of impact response region (μs)	172.5	170.0	167.2
Maximum amplitude of impact response region	591.41	71.88	649.44
Duration of vibrational response region (μs)	273	180.5	334.2
Maximum amplitude of vibrational response region	437.86	118.92	476.87
Dominant frequency (kHz)	11.6	7.0	11.0

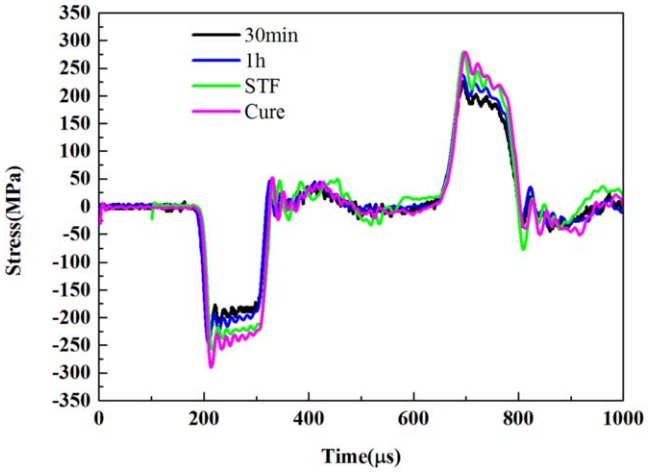

Figure 9. Stress waves of 300 mm projectile impacting incident bar with epoxy resins with different curing times.

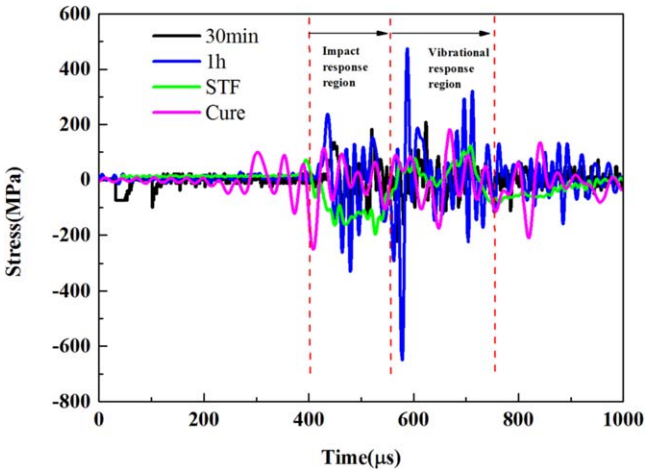

Figure 10. Comparison of axial strain in flange with STFs and three epoxy resins with different curing times.

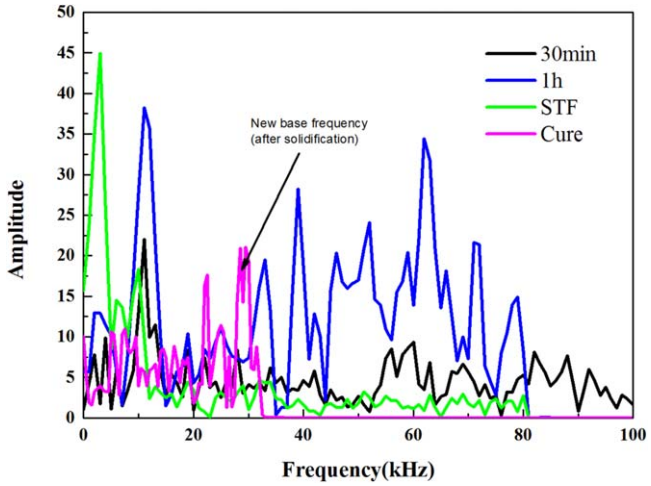

Figure 11. FFT spectrums of fillers: STFs, and three epoxy resins with different curing times.

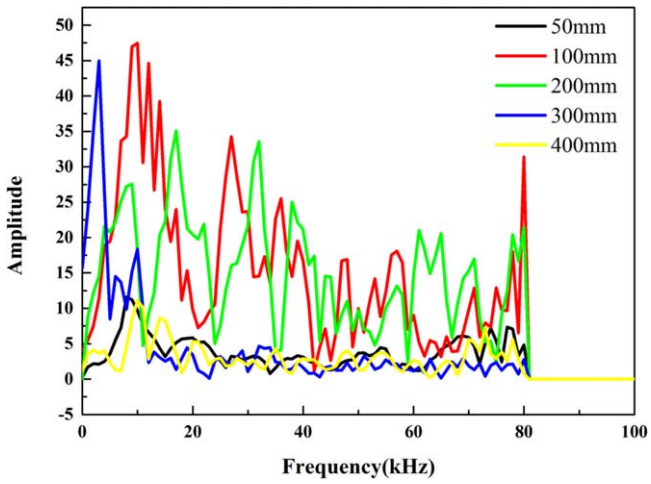

Figure 12. FFT spectrum under different impact pulse widths.

of both regions are found at the case of 100 mm. A_p represents the amplitude of impact response region and A_v for vibrational response region, while A_0 is the loading amplitude. We have been studied the natural frequency of flange structure without fillers and the dominant frequency was 11 KHz. This base frequency was derived from modal analysis by ABAQUS. Experimental results also confirmed that. STFs remains mixture fluid-solid state, making it hard to derive natural frequency. Nevertheless, the dominant frequency may slightly change due to unsolidified fillers, in this paper, 11 KHz is still regard as the natural frequency. When the pulse width of excitation increases, the amplitude decreases. Because STFs can absorb most energies, in the case of 400 mm the oscillation is hardly excited. The duration of the vibrational region continues decreasing as the pulse width of excitation is gradually increased, and is similar to previous studies. Our previous study found that the duration of vibrational response region diminished when the frequency

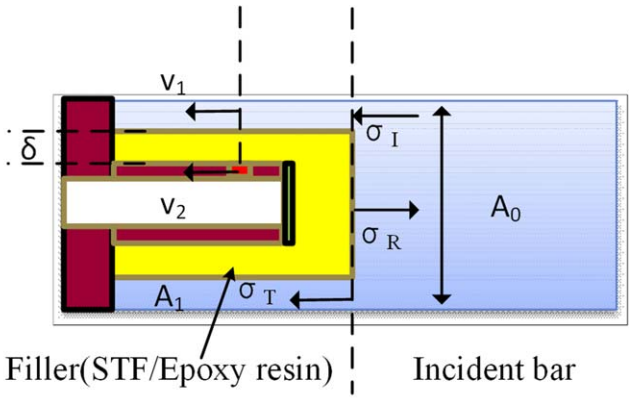

Figure 13. The diagram calculating shear rate of flange structures with fillers.

of excitation became lower for the original flange without fillers. Energy received by the flange indicates that moderate excitation contributes little power to generate vibrations. However, in the case of 300 mm, the duration of the vibrational response region did not decrease as expected. The FFT spectrum shown in figure 12 exhibits the same phenomenon. The dominant frequency is significantly less with 300 mm loading, and on the contrary, most of the cases concentrate the energy at 10.0 kHz. It may correlate to the shear rate and the description will be discussed in the following part. It appears as if the energy received by the flange is significantly smaller in the 300 mm case. In addition, the effective energy absorption of STF reduces vibration suppression.

Considering the difficulties to predict stress-waves after it spread across the end of the bar, only the first transmitted wave is discussed. Sequent noises, reflection and dissipation of the flange is not conducted. As figure 13, V_1 is the particle velocity of incident bar and V_2 is the velocity of measure point. It is also the particle velocity of the flange. According to the definition of shear rate, we can get the formulae to calculate shear rate $\dot{\gamma}$,

$$\dot{\gamma} = v/\delta = V_2 - V_1/\delta \tag{2}$$

where δ is the thickness of STFs layer. V_2 is the measuring signal, while V_1 should be derived from the wave analysis. The incident bar has a variable cross-section. Stress wave may reflect at the interface. Therefore, we can get the reflected wave and transmitted wave for the variable cross-section,

$$A_0(\sigma_I + \sigma_R) = A_1\sigma_T \tag{3}$$

where A_0 is the original surface area of incident bar, and A_1 is the surface area of slim cylinder. σ_I represents the incident wave, while σ_R and σ_T are the reflected wave and transmitted wave respectively. Once we derived the transmitted wave, based on the relationship of velocity and stress, V_1 is described as,

$$V_1 = \sigma_T/(\rho_0 C_0) \tag{4}$$

where ρ_0 and C_0 are the density and wave speed of steels. There is a distance between the point of the incident bar right above measuring point and the interface. Thus, the stress wave may be delayed a few seconds. The shear rates under various pulse width of impact are shown in figure 14.

In the case of 100 mm, the shear rate reach its maximum 12000 s^{-1}. Therefore, STFs are the most effective in preventing vibration. The amplitudes in both regions are quite large, 0.62 and 0.33. The structure probably resonate. The pulse width of 100 mm loading mainly is 60 μs, a little bigger than 45 μs. Resonation occurs when the loading frequency is just 11 KHz. In the case of 300 mm, the shear rate starts to decrease after 100 μs. It means the drive force of shear thickening phenomenon continuously diminishes. As a result, the duration of vibrational response region is larger than the others. In the case of 400 mm, although the shear rate is almost the same as that in case 300 mm, the pulse width of loading increases much more. Moderate impulses can hardly excite oscillations and the nonlinear response is attenuated.

3.4. Transmission ratio under different excitation

Different pulse widths of excitations impacting joints with STF protection are discussed in this section, and the impact resistance is also evaluated. Axial strains of the flange subjected to various durations of square shockwaves are shown in a figure 15. The length of projectiles ranges from 50 mm–400 mm. Loading stresses range from 222.56 Mpa–251.29 Mpa. As figure 16, we can acquire the mean stress of plateau. Significant oscillation is exhibited in the case of 200 mm, however, other durations indicated that STF has significant vibration attenuating effects. Our previous study reported that greater impacts generated greater nonlinearities, while impulses with long pulse widths gradually approached the quasi-static loading state [2]. This phenomenon is defined as the transmission ratio α, that represents the degree of distortion in shockwaves crossing bolted flange joints, and is also prominent in experiments with STF protectors. The change of the transmission ratio from greater than 1.6 to 1.0, as the excitation pulse width increases, is shown in figure 17. The horizontal axis is the dimensionless time of the pulse width of loading to the natural period of the structure. The vertical axis means the dimensionless time of the duration of impact response region to the pulse width of loading. The latter is also defined as the transmission ratio. The data from joints with STFs lies immediately below previous simulation results, confirming that the impact resistance of STFs shortens the duration of the impact response region.

4. Conclusions

This study focused on the impact resistance of bolted flange structures stuffed with STFs under various impacts. The study was conducted using a modified SHPB platform, applying 7 m s^{-1}–14 m s^{-1} impact velocities, and five different pulse widths. In order to prove the excellent capacity of STFs in preventing oscillation, the flange structure both without fillers and with proxy resin fillers were also investigated. Different pulse widths of excitation were used to evaluate the impact resistance of STFs. Durations and amplitudes in both regions

Table 4. Detailed experimental data of five impact pulse widths (STFs cases).

Lengths of projectiles (mm)	50	100	200	300	400
Maximum amplitude of impact response region (A_P/A_0)	0.14	0.62	0.51	0.19	0.12
Duration of vibrational response region (μs)	398.4	335.4	261.0	384.2	192.6
Maximum amplitude of vibrational response region (A_V/A_0)	0.10	0.33	0.20	0.12	0.10
Dominant frequency (kHz)	8.0	10.0	17.0	3.0	10.0

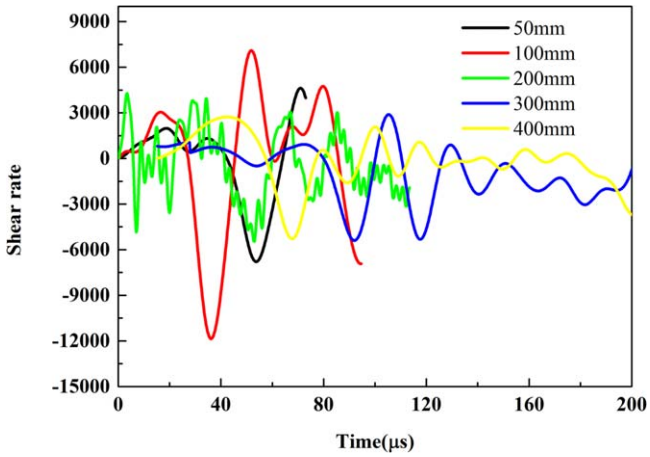

Figure 14 The shear rate under different pulse width impacts.

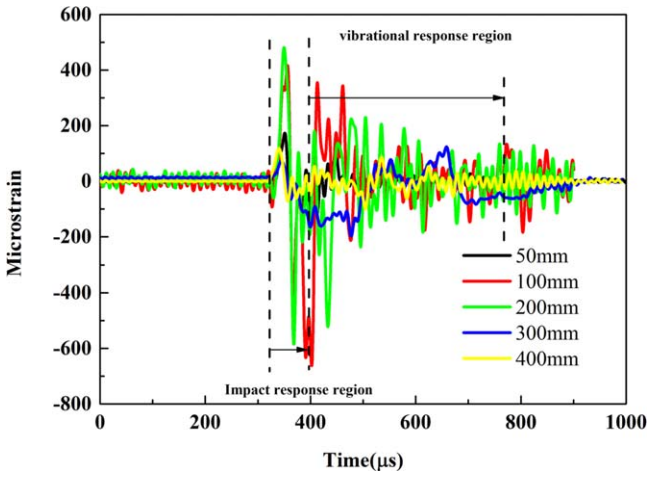

Figure 15. Axial strains of flange with STF protection subjected to different pulse widths of impacts.

were key characteristics for evaluating the efficiency of STFs. Vibrations were compared with dominant frequencies.

1. Experimental results indicated that STFs clearly damped the amplitude of tail strain, and shortened the duration of vibrational response regions. In addition, the dominant frequency in the STF case was reduced compared to structures without fillers or stuffed with epoxy resins.
2. Epoxy resins with different curing times were studied to prove the efficacy of STFs. The results indicated that STFs exhibited positive vibrational suppression, not only inhibiting the high frequency oscillations caused by shockwaves spreading in the flange, but also decreased the base frequency of the structure, suggesting the feasibility of substituting proxy resins as embedding material in engineering applications.
3. The STFs could suppress vibrations of high frequency under different levels of excitation, and were validated with wave pulse widths from 50 mm–400 mm. The amplitudes of both regions attained a maximum at 100 mm case, and that suggested structural resonance. Shear rates of STFs under different pulse widths of excitation were also discussed, explaining the extinct behavior of case 300 mm.

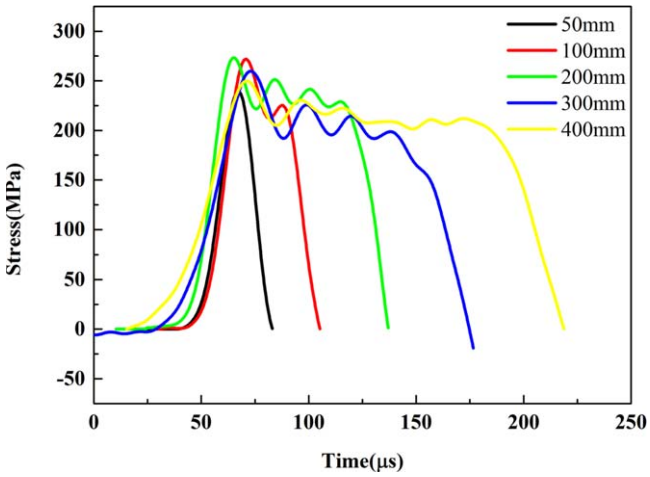

Figure 16. Loading stress of flange with STFs subjected to different pulse widths of impacts.

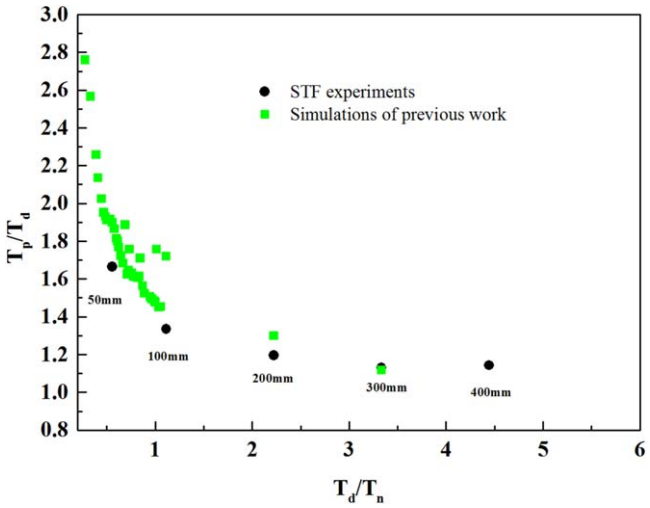

Figure 17. Transmission ratio at different impact pulse widths.

4. The force transmission ratios of the different cases were similar, irrespective of the filler that accurately reflected the actual loading information. The transmission ratio decreased with decreasing excitation, which is similar to the regulation of joints without protectors.

Acknowledgments

The authors would like to thank the National Natural Science Foundation of China [Grant no.11502274, 11002150, 11332011, 11402277] and the Basic Research Equipment Project of the Chinese Academy of Sciences [YZ200930] for financial support.

ORCID iDs

Yanpeng Wei https://orcid.org/0000-0001-6435-2126

Reference

[1] Abid M and Nash D H 2006 Structural strength: gasketed vs non-gasketed flange joint under bolt up and operating condition *International Journal of Solids & Structures* **43** 4616–29
[2] Guo Y, Wei Y, Yang Z, Huang C, Wu X and Yin Q 2017 Nonlinearity of interfaces and force transmission of bolted flange joints under impact loading *Int. J. Impact Eng.* **109**
[3] Iyer S S, Vedad-Ghavami R, Lee H, Liger M, Kavehpour H P and Candler R N 2013 Nonlinear damping for vibration isolation of microsystems using shear thickening fluid *Appl. Phys. Lett.* **102** 251902
[4] Sherwood J A and Frost C C 1992 Constitutive modeling and simulation of energy absorbing polyurethane foam under impact loading *Polymer Engineering & Science* **32** 1138–46
[5] Payne A R 1962 The dynamic properties of carbon black-loaded natural rubber vulcanizates *Part I, Journal of Applied Polymer Science* **6** 57–63
[6] Sarlin E, Apostol M, Lindroos M, Kuokkala V T, Vuorinen J, Lepist T O and Vippola M 2014 Impact properties of novel corrosion resistant hybrid structures *International Journal of Adhesion & Adhesives* **49** 51–7
[7] Zhang X Z, Li W H and Gong X L 2008 The rheology of shear thickening fluid (STF) and the dynamic performance of an STF-filled damper *Smart Mater. Struct.* **17** 035027
[8] Lee Y-S and Wagner N 2003 Dynamic properties of shear thickening colloidal suspensions *Rheologica Acta* **42** 199–208
[9] Bender J and Wagner N J 1996 Reversible shear thickening in monodisperse and bidisperse colloidal dispersions *J. Rheol.* **40** 899–916
[10] Jiang W, Gong X, Xuan S, Jiang W, Ye F, Li X and Liu T 2013 Stress pulse attenuation in shear thickening fluid *Appl. Phys. Lett.* **102** 101901
[11] Waitukaitis S R and Jaeger H M 2012 Impact-activated solidification of dense suspensions via dynamic jamming fronts *Nature* **487** 205–9
[12] Laun H M, Bung R and Schmidt F 1991 Rheology of extremely shear thickening polymer dispersionsa) (passively viscosity switching fluids) *Journal of Rheology (1978-present)* **35** 999–1034
[13] Boersma W H, Laven J and Stein H N 1992 Viscoelastic properties of concentrated shear-thickening dispersions *Journal of Colloid & Interface Science* **149** 10–22
[14] Zhang X, Li W and Gong X L 2008 Study on magnetorheological shear thickening fluid *Smart Mater. Struct.* **17** 015051
[15] Raghavan S R and Khan S A 1997 Shear-thickening response of fumed silica suspensions under steady and oscillatory shear *Journal of Colloid & Interface Science* **185** 57–67
[16] Lim A S, Lopatnikov S L, Wagner N J and Gillespie J W 2010 Investigating the transient response of a shear thickening fluid using the split Hopkinson pressure bar technique *Rheol. Acta* **49** 879–90
[17] Wu X, Zhong F, Yin Q and Huang C 2015 Dynamic response of shear thickening fluid under laser induced shock *Appl. Phys. Lett.* **106** 071903
[18] Wu X, Yin Q and Huang C 2015 Experimental study on pressure, stress state, and temperature-dependent dynamic behavior of shear thickening fluid subjected to laser induced shock *J. Appl. Phys.* **118** 173102
[19] Helber R, Doncker F and Bung R 1990 Vibration attenuation by passive stiffness switching mounts *J. Sound Vib.* **138** 47–57
[20] Decker M J, Halbach C J, Nam C H, Wagner N J and Wetzel E D 2007 Stab resistance of shear thickening fluid (STF)-treated fabrics *Compos. Sci. Technol.* **67** 565–78
[21] Fischer C, Bennani A, Michaud V, Jacquelin E and Månson J-A E 2010 Structural damping of model sandwich structures using tailored shear thickening fluid compositions *Smart Mater. Struct.* **19** 035017
[22] Lee Y S, Wetzel E D and Wagner N J 2003 The ballistic impact characteristics of kevlar woven fabrics impregnated with a colloidal shear thickening fluid *J. Mater. Sci.* **38** 2825–33
[23] Tan V B C, Tay T E and Teo W K 2005 Strengthening fabric armour with silica colloidal suspensions *Int. J. Solids Struct.* **42** 1561–76
[24] Fischer C, Braun S A, Bourban P E, Michaud V, Plummer C J G and Månson J A E 2006 Dynamic properties of sandwich structures with integrated shear-thickening fluids *Smart Mater. Struct.* **15** 1467–75
[25] Wei M, Hu G, Jin L, Lin K and Zou D 2016 Forced vibration of a shear thickening fluid sandwich beam *Smart Mater. Struct.* **25** 055041
[26] Somasundaram D S, Trabia M B and O'Toole B J 2014 A methodology for predicting high impact shock propagation within bolted-joint structures *Int. J. Impact Eng.* **73** 30–42
[27] Garschke C, Parlevliet P P, Weimer C and Fox B L 2013 Cure kinetics and viscosity modelling of a high-performance epoxy resin film *Polym. Test.* **32** 150–7
[28] Kiuna N, Lawrence C J, Fontana Q P V, Lee P D, Selerland T and Spelt P D M 2002 A model for resin viscosity during cure in the resin transfer moulding process *Composites Part A Applied Science & Manufacturing* **33** 1497–503
[29] Lapique F and Redford K 2002 Curing effects on viscosity and mechanical properties of a commercial epoxy resin adhesive *International Journal of Adhesion & Adhesives* **22** 337–46
[30] Enns J B and Gillham J K 1983 *J. Appl. Polymer Sci.* **28** 2567–91
[31] Esteban J, Lalande F, Rogers C and Chaudhry Z 1996 Theoretical modeling of wave propagation and energy dissipation in joints *AIAA Adaptive Structures Forum 1996* pp 131–41
[32] Mewis J and Biebaut G 2001 Shear thickening in steady and superposition flows effect of particle interaction forces *J. Rheol.* **45** 799–813